

Statistical modeling of monthly streamflow using time series and artificial neural network models: Hindiya Barrage as a case study

Nabeel H. Al-Saati^a, Isam I. Omran^a, Alaa Ali Salman^a, Zainab Al-Saati^a and Khalid S. Hashim^{b,c,*}

^a Al-Mussaib Technical Institute, Al-Furat Al-Awsat Technical University, Babylon 51009, Iraq

^b Department of Environment Engineering, Babylon University, Babylon 51001, Iraq

^c School of Civil Engineering and Built Environment, Liverpool John Moores University, Liverpool, UK

*Corresponding author. E-mail: khalid_alhilli@yahoo.com

Abstract

Autoregressive Integrated Moving Average (ARIMA) Box-Jenkins models combine the autoregressive and moving average models to a stationary time series after the appropriate transformation, while the nonlinear autoregressive (N.A.R.) or the autoregressive neural network (ARNN) models are of the kind of multi-layer perceptron (M.L.P.), which compose an input layer, hidden layer and an output layer. Monthly streamflow at the downstream of the Euphrates River (Hindiya Barrage) /Iraq for the period January 2000 to December 2019 was modeled utilizing ARIMA and N.A.R. time series models. The predicted Box-Jenkins model was ARIMA (1,1,0) (0,1,1), while the predicted artificial neural network (N.A.R.) model was (M.L.P. 1-3-1). The results of the study indicate that the traditional Box-Jenkins model was more accurate than the N.A.R. model in modeling the monthly streamflow of the studied case. Performing a one-step-ahead forecast during the year 2019, the forecast accuracy between the forecasted and recorded monthly streamflow for both models was as follows: the Box-Jenkins model gave root mean squared error (RMSE = 48.7) and the coefficient of determination ($R^2 = 0.801$), while the (NAR) model gave (RMSE = 93.4) and ($R^2 = 0.269$). Future projection of the monthly stream flow through the year 2025, utilizing the Box-Jenkins model, indicated the existence of long-term periodicity.

Key words: ANN, Box-Jenkins, monthly stream flow, RMSE, time series

Highlights

- Box-Jenkins models and artificial neural network (ANN) were used to model the flow of Hindiya Barrage.
- The collected data covered the period of January 2000 to December 2019.
- Box-Jenkins model was more accurate than ANN in modeling the monthly flow of the studied river.
- The outcomes indicated long-term periodicity (until 2025).

INTRODUCTION

Streamflow is an important issue in the design, operation, and control of many vital projects in the water resources and sanitary/environmental engineering specialities; examples are reservoir storage capacity, water treatment plants (WTPs), and wastewater treatment plants (WWTPs). For this reason, recorded data of streamflow (hourly, daily, weekly, monthly, and yearly) are required

This is an Open Access article distributed under the terms of the Creative Commons Attribution Licence (CC BY-NC-ND 4.0), which permits copying and redistribution for non-commercial purposes with no derivatives, provided the original work is properly cited (<http://creativecommons.org/licenses/by-nc-nd/4.0/>).

for the optimum design, operation, and control of these vital projects. Kawamura (2000) showed that during the preliminary studies to design a (WTP), the project engineer must evaluate the potential sources of water; one of the elements of this evaluation is the quantity of water required, which is directly related to the streamflow of the nearby river (delivering raw water). The importance of streamflow in the design, operation, and control of a WWTP is best illustrated by the direct relation between the self-purification of rivers to the river streamflow (as shown in the Streeter-Phelps equation) and the direct effect of the dilution factor (Metcalf *et al.* 1979). Monthly streamflow of the Sefidrood river, Iran, and Sangeen river, Canada, were studied and modeled by applying autoregressive (AR), moving average (MA) models and compared with two artificial intelligence (AI) approaches, namely, multivariate adaptive regression splines (MARS) and gene expression programming (GEP). Results indicate that AI models outperformed the conventional AR and MA models (Mehdizadeh *et al.* 2019). Frausto-Solis *et al.* (2008) compared ARIMA versus ANN in forecasting streamflow. Their results indicate that ARIMA has a higher forecast accuracy than ANN methodology. Moeeni *et al.* (2017) compared the Seasonal Autoregressive Integrated Moving Average (SARIMA) with the Artificial Neural Network-Genetic Algorithm (ANN-GA) method in forecasting the monthly streamflow. Their results confirm that the SARIMA model have much more accuracy than the ANN-GA model in short-term and long-term forecasting. Joodavi *et al.* (2020) presented a methodology based on the combination of numerical groundwater flow simulations and reservoir operation optimization models to develop an optimization model for the management of the off-stream Bar-Reservoir operation (Iran), taking into account the lake bed seepage and the random inflow to the reservoir, the planned objective was to satisfy water demand for a total amount of 12 million m³/year for drinking and industrial purposes. A two-stage time series model for the monthly flows of the Lim River basin in South-Eastern Europe for the period 1950–2012 was carried out by Stojković *et al.* (2020). The model took into consideration climate change and consisted of several components (trend, long-term periodicity, seasonality, and the stochastic component). It was designed to estimate future water availability. Water demand of any city varies according to the variation of climatic variables (Zubaidi *et al.* 2020a, 2020b, 2020c), such as rainfall, temperature, humidity, and evaporation (Zubaidi *et al.* 2019a, 2019b, 2020d, 2020e). Feng & Niu (2021) proposed a hybrid artificial neural network model enhanced by the addition of a cooperation search algorithm for nonlinear river stream flow time series forecasting. Mohammadi *et al.* (2020) developed novel robust models to improve the accuracy of daily streamflow time series modeling. Niu & Feng (2021) evaluated the performance of five artificial intelligence models in forecasting the daily streamflow time series. Adnan *et al.* (2020) evaluated the abilities of three models to predict monthly streamflow; they are Group Method of Data Handling-Neural Networks (GMDH-NN), Dynamic Evolving Neural-Fuzzy Inference System (DENFIS), and Multivariate Adaptive Regression Spline (MARS) methods. Peng *et al.* (2020) developed a monthly streamflow prediction model based on the Random Forest Algorithm and Phase Space Reconstruction Theory. Khazaei *et al.* (2020) simulated daily runoff correlated to weather generators utilizing the LARS-WG model. Avand & Moradi (2020) used machine learning models (including LARS-WG), remote sensing, and GIS to study the effects of changing climatic variables and land uses on flood probability.

To the best of the authors' knowledge, this is the first time that statistical modeling models were built for monthly streamflow at the Euphrates River (Hindiya Barrage) in Iraq. Generally, this paper aims to firstly investigate the monthly streamflow at downstream of the Euphrates River (Hindiya Barrage) /Iraq for the period of January 2000 to December 2018. Secondly, building a Box-Jenkins ARIMA forecasting model for the data recorded during the above period, checking its adequacy and proving its goodness of fit. Then, performing a one-step-ahead forecast during the year 2019 (12 months). Thirdly, train, test and validate the above-recorded data using the multi-layer perceptron (MLP) and feed-forward neural network (FNN). Then performing a one-step-ahead forecast during the year 2019 (12 months). Finally, compare the forecast accuracy for the two methods relying on the root mean squared error (RMSE)

and the coefficient of determination (R^2). Average monthly streamflow data at the downstream of the Euphrates River (Hindiya Barrage), Iraq for the period January 2000 to December 2019 were selected as a case study (these data were obtained from the Ministry of Water Resources/Al-Mussaib Water Resources Directorate, Iraq). The data for the period 2000–2018 was adopted in model building and that during 2019 were adopted for calculating model forecast accuracy.

Figure 1 is an aerial view (Google Earth) of the study area with Latitude $32^{\circ}43'01''$ N, Longitude $44^{\circ}16'01''$ E.

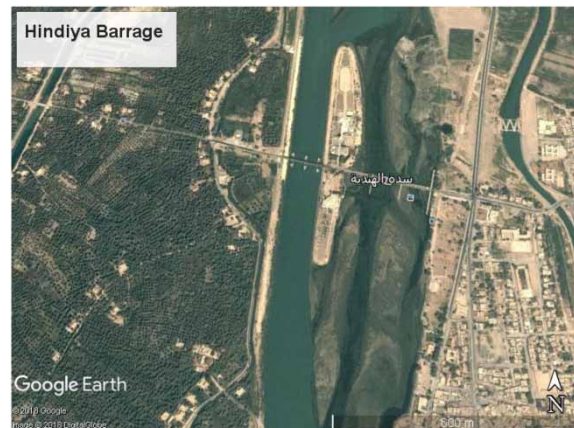


Figure 1 | Aerial view of Hindiya Barrage.

MATERIALS AND METHODS

Univariate Box-Jenkins ARIMA family of time series models

A time series of a finite number of successive observations consisting of the data $Y_1, Y_2, \dots, Y_{t-1}, Y_t, Y_{t+1}, \dots, Y_n$ is called a univariate time series. Autoregressive Integrated Moving Average (ARIMA) models describe a collection of time series models that can be very simple or complicated (Brown & Mac Berthouex 2002). A seasonal ARIMA model for Y_t is written as (Geurts 1977):

$$\theta(B)\varphi(B^S)(\nabla^d \nabla_S^D Y_t^\lambda - \mu) = \theta(B)\psi(B^S)a_t \quad (1)$$

where Y_t^λ represent some appropriate transformation of Y_t , t is the discrete-time, S is the seasonal length (equals 12 for monthly data), B is the backshift operator defined by $BY_t = Y_{t-1}$ and $B^S Y_t = Y_{t-S}$, μ is the mean level of the series, usually taken as the average of the W_i series (if $D + d > 0$, often $\mu \cong 0$), a_t is normally independently distributed white noise series (no autocorrelation) (with mean = 0 and variance = σ_a^2 , it is written as NID (0, σ_a^2)).

$$\Theta(B) = 1 - \Theta_1 B - \Theta_2 B^2 \dots \dots \dots - \Theta_P B^P \quad (2)$$

where $\Theta(B)$ is a non-seasonal autoregressive (AR) operator of order (P).

$$\Phi(B^S) = 1 - \Phi_1 B^S - \Phi_2 B^{2S} \dots \dots \dots - \Phi_P B^{PS} \quad (3)$$

where $\Phi(B^S)$ is the seasonal AR operator of order (P), ∇^d = non-seasonal differencing operator of order (d) to produce non-seasonal stationarity (trend removal), usually $d = 0, 1$ or 2 , ∇_S^D = seasonal

differencing operator of order (D) to produce seasonal stationarity (seasonality removal), usually $D = 0, 1$ or 2 .

$$\theta(B) = 1 - \theta_1 B - \theta_2 B^2 \dots \dots \dots - \theta_q B^q \tag{4}$$

where $\theta(B)$ = non-seasonal moving average (MA) operator of order(q).

$$\psi(B^S) = 1 - \psi_1 B^S - \psi_2 B^{2S} \dots \dots \dots - \psi_Q B^{QS} \tag{5}$$

where $\psi(B^S)$ = seasonal (MA) operator of order (Q), and W_t = stationary time series formed by non-seasonal and/or seasonal differencing of Y_t^λ time-series. ARIMA models (Box *et al.* 2015) can handle the problem of statistical modeling of any time-dependent phenomenon, including model building, forecasting and diagnostic checking, taking into account stationarity, missing data, outlier observations, intervention, normality, and independence of residuals. A stationary time series is defined as a time series without trend and seasonality; that is, with zero mean and small variance (Box *et al.* 2015). For the precise explanation of the three steps of model building (identification, estimation, and diagnostic check), the interested reader may refer to (Ljung & Box 1978; Ang & Tang 2007). The above three steps of Box-Jenkins ARIMA modeling (model building, forecasting and diagnostic checking) can be easily executed using IBM SPSS version 20 software (Yaffee & McGee 2000).

Artificial neural network (ANN) models

The recommended modeling procedure here, according to the published literature (Faraway & Chatfield 1998; Tealab *et al.* 2017), is the nonlinear autoregressive (NAR) or the autoregressive neural network (ARNN). It is of the kind of multi-layer perceptron (MLP), which comprises an input layer, hidden layer and an output layer. The input layer holds the target vector (time series), while the output layer computes the estimator vector (time series). The hidden and output layers are governed by an activation function, which may be defined by a (logistic, tanh, softmax...), and a weight function (uniform and Gaussian). Figure 2 is a schematic representation of a perceptron learning process.

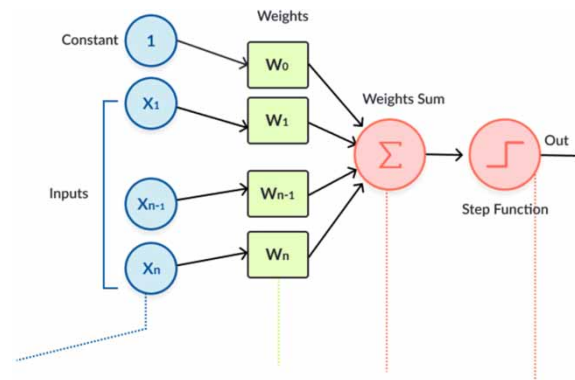


Figure 2 | Perceptron learning process.

The nonlinear autoregressive model of order p, NAR (p), is defined as:

$$Y_t = h(Y_{t-1}, \dots, Y_{t-p}) + \varepsilon_t \tag{6}$$

where $h(\cdot)$ is a nonlinear function; it is assumed that (ε_t) is a sequence of random independent variables and identically distributed with zero mean and a finite variance σ^2 . The ARNN is a feed-forward

network that constitutes a nonlinear approximation $h(\cdot)$, which is defined as:

$$\hat{Y}_t = \hat{h}(Y_{t-1}, \dots, Y_{t-p}) \quad (7)$$

$$\hat{Y}_t = \beta_0 + \sum_{i=1}^I \beta_i f \left(\alpha_i + \sum_{j=1}^p \omega_{ij} Y_{t-j} \right) \quad (8)$$

where $f(\cdot)$ function is the activation function and $\theta = (\beta_0, \beta_1, \dots, \beta_q, \alpha_1, \dots, \alpha_q, \omega_{11}, \dots, \omega_{qn})$ is the parameter vector of the neural network, which is calculated by minimizing the sum of squared errors:

$$SSE = \sum_{t=1}^n (Y_t - \hat{Y}_t)^2 \quad (9)$$

where \hat{Y}_t is the estimator of the target variable Y_t . The recorded data (for the purpose of analysis) is divided into three portions, N_1 , N_2 and N_3 . N_1 of the data are used for training. N_2 are used for data validation to check the prediction accuracy for the model selection. N_3 of the data are employed for the out-of-sample predictions (forecasts) by the calibrated model. The smallest number of RMSEs for the validation data becomes a desirable model (Kajitani *et al.* 2005). During the training stage, several algorithms were adopted for optimization and truncating the iterations (cycles) after reaching the specified error criteria, strictly speaking, Broyden-Fletcher-Goldfarb-Shanno (BFGS), Scaled Conjugate and Gradient Descent algorithms (Bishop 1995; Becerikli *et al.* 2003). The model that gives the maximum correlation coefficient (R) and the minimum sum of squared errors (SSE) will be relied on in the analysis (KİŞİ & Sciences 2005). The above modeling procedure was performed and analyzed in this research adopting STATISTICA version 12 software.

Forecasting

After model building, it is necessary to make a one-step-ahead forecast. To check the forecasting accuracy, several formulas are calculated and checked according to the forecast accuracy, these are coefficient of determination (R^2), root mean squared error (RMSE), mean absolute error (MAE), mean absolute percentage error (MAPE), maximum absolute error (MaxAE), and maximum absolute percentage error (MaxAPE). The above formulas can be found in any statistical textbook. For example, to define (RMSE) and R^2 , then:

$$RMSE = \sqrt{\frac{\sum_{t=1}^N (Y_t - F_t)^2}{N}} \quad (10)$$

$$R^2 = 1 - \frac{SS_{res}}{SS_{tot}} \quad (11)$$

$$SS_{res} = \sum_{t=1}^N (Y_t - F_t)^2 = \sum_{t=1}^N (E_t)^2 \quad (12)$$

$$SS_{tot} = \sum_{t=1}^N (Y_t - \bar{Y})^2 \quad (13)$$

where N = the number of months to be forecasted in the future (normally 12), Y_t = observed (recorded) stream flow at month t (m^3/s), F_t = forecasted streamflow at month t (m^3/s), \bar{Y} = average

of observed values (m^3/s), \bar{F} = average of forecasted values (m^3/s), E_t = error (residual) at time t (m^3/s). These accuracy formulas are calculated and updated from the same recommended software, IBM SPSS version 20 and STATISTICA version 12.

RESULTS AND DISCUSSION

Applying the Box-Jenkins modeling procedure to the recorded data, using IBM SPSS version 20 software referring to the route (Analyze/Forecasting/Create Models/Expert Modeler), the best-fit model relying on the RMSE criteria was: ARIMA (1,1,0) (0,1,1).

The appropriate equation was:

$$(1 + 0.174B)\nabla^1 \nabla_{12}^1 \ln \hat{Y}_t = (1 - 0.951B^{12})a_t \quad (14)$$

The original data suggested a natural logarithmic transformation to enhance the normality of residuals. The above model gave $R^2 = 0.844$, $RMSE = 42.049$ and Ljung-Box $Q(18) = 21.906$ with degrees of freedom (DF) = 16, also the significance of Q was $14.6\% > 5\%$, indicating that residuals from the model were uncorrelated (random). Figure 3 depicts the autocorrelation function (ACF) and partial autocorrelation function (PACF) of the residuals. Figure 4 depicts the normal probability paper of the residuals.

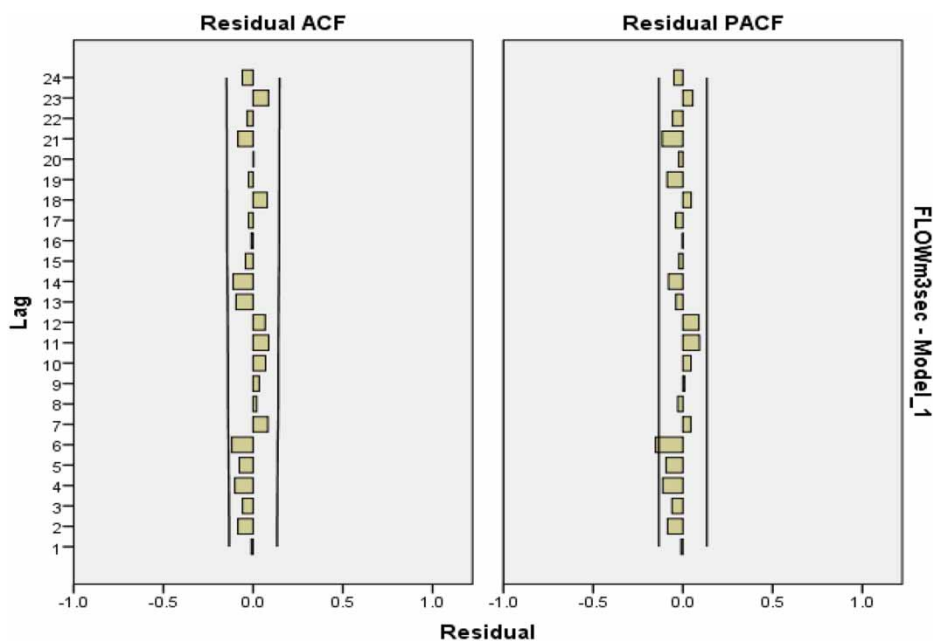


Figure 3 | ACF and PACF of the residuals.

From the above figures, it is evident that the residuals are normally independently distributed. Figure 5 describes the predicted values of the streamflow time series together with the recorded values. It states that there was a clear, strong correlation between predicted and recorded values.

Figure 6 depicts the forecasted monthly streamflow for the 12 months during 2019, together with the recorded values. The calculated $RMSE = 48.7$ and the calculated $R^2 = 0.801$.

Applying the (ANN) modeling procedure to the above data using the STATISTICA version 12 software, referring to the route (Data Mining/Neural Networks/Time Series (Regression)), taking into consideration that the recorded data was considered as the Target, the input layer was taken as the

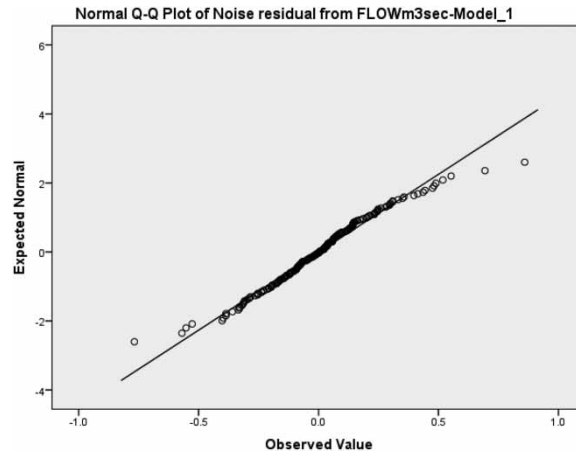


Figure 4 | Normal probability paper of the residuals.

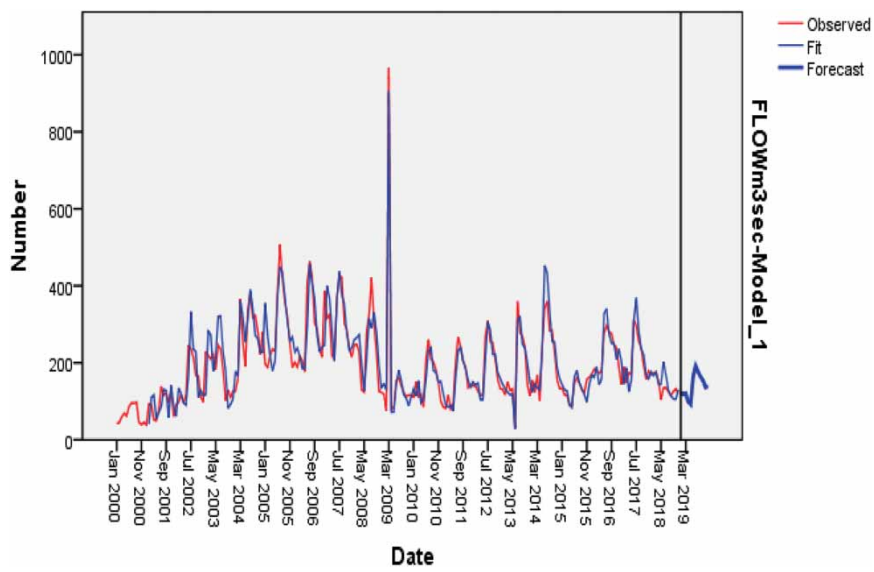


Figure 5 | Box-Jenkins ARIMA model predicted time series vs. recorded time series for the period 2000–2018.

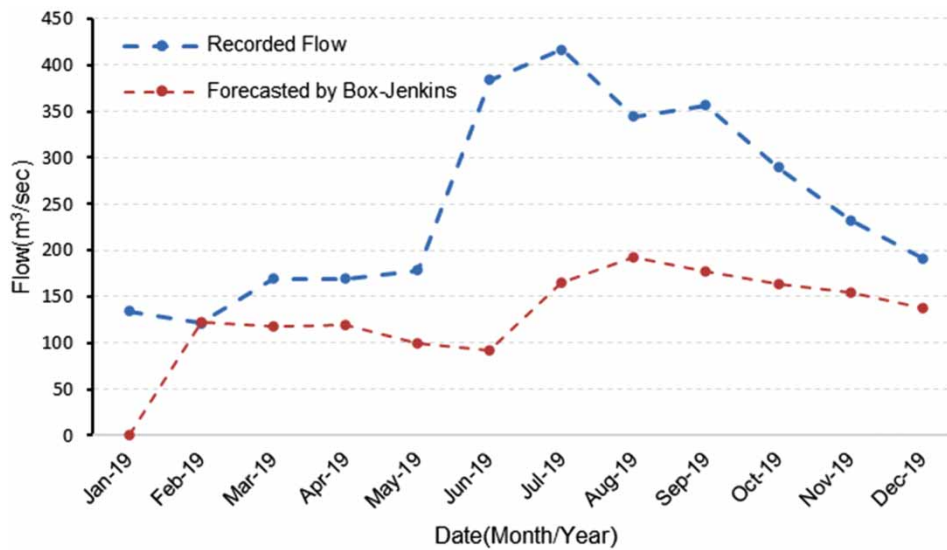


Figure 6 | Recorded vs. Forecasted (by Box-Jenkins) monthly stream flow during 2019.

Target with a lag of specified length, the input layer data were classified as (70% Training + 15% Test + 15% Validation) randomly. The results in the output layer will be compared with the target. Table 1 lists the statistics of the predicted ANN models for different lags between (1–12), noting that one cycle of seasonality = 12 months.

Table 1 | Showing statistics of the predicted ANN models

Lag	Predicted model	Training (R)	Test (R)	Validation (R)	Training (S.S.E.)	Test (S.S.E.)	Validation (S.S.E.)	Training algorithm
1	MLP 1-3-1	0.560163	0.651468	0.898259	4,257.256	3,018.890	821.1875	BFGS 4
2	MLP 2-6-1	0.544030	0.435790	0.868627	5,330.841	4,504.276	2,921.298	BFGS 2
3	MLP 3-2-1	0.601277	0.735790	0.860533	3,917.588	2,356.384	919.7809	BFGS 35
4	MLP 4-8-1	0.616656	0.756074	0.867327	3,765.428	2,182.703	864.7852	BFGS 34
5	MLP 5-5-1	0.518009	0.519080	0.816368	4,448.370	4,219.433	1,246.969	BFGS 3
6	MLP 6-2-1	0.614488	0.729865	0.800189	3,755.190	2,356.035	1,026.629	BFGS 41
7	MLP 7-7-1	0.662119	0.706750	0.796674	3,394.344	2,612.846	1,170.198	BFGS 35
8	MLP 8-3-1	0.657709	0.637734	0.784143	3,426.545	3,208.390	1,128.715	BFGS 38
9	M.L.P. 9-6-1	0.548164	0.650932	0.846927	4,201.155	2,708.997	909.2035	BFGS 7
10	MLP 10-4-1	0.498419	0.499938	0.743900	4,498.307	3,813.725	1,191.457	BFGS 5
11	MLP 11-6-1	0.533244	0.475782	0.759208	4,305.496	3,775.697	1,342.761	BFGS 7
12	MLP 12-8-1	0.494050	0.656991	0.723700	4,364.795	2,680.175	1,302.532	BFGS 3

Table 1 reflects the fact that all predicted models are not strongly correlated with the Target, indicating a small coefficient of determination (R^2). It is evident from Table 1 that the maximum (R) and the minimum SSE (validation stage) occurred at lag 1 (MLP 1-3-1); for this, it is selected as the best model. The notation (MLP 1-3-1), for example, refers to a multi-layer perceptron with 1 (number of inputs), 3 (number of hidden units), and 1 (number of outputs); also, the notation BFGS 4 refers to the Broyden-Fletcher-Goldfarb-Shanno training algorithm with 4 cycles of iteration. Figure 7 is a time-series graph that compares the prediction of the model at lag 1 (MLP 1-3-1) with the recorded data (Target). Figure 8 compares the (Target) streamflow Q (x-axis) with the output streamflow

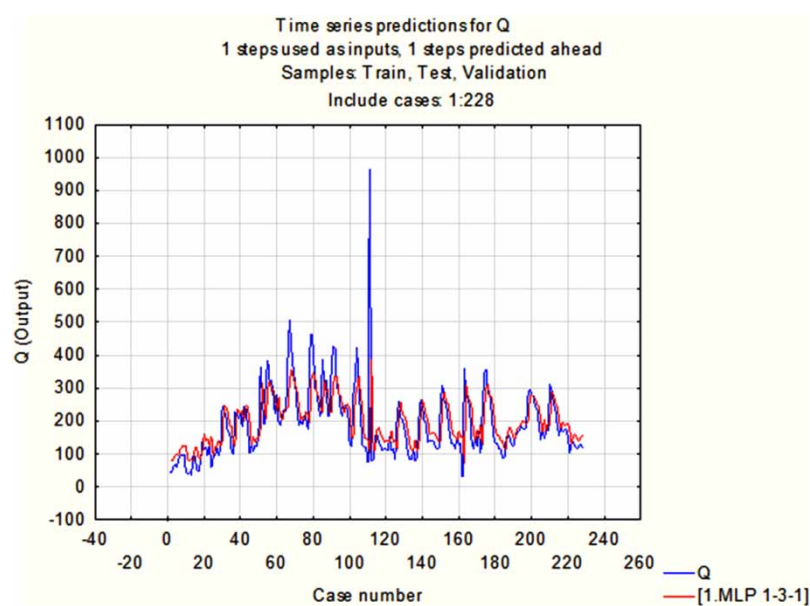


Figure 7 | Predictions of the ANN model (MLP 1-3-1) compared to the recorded data for the period 2000–2018.

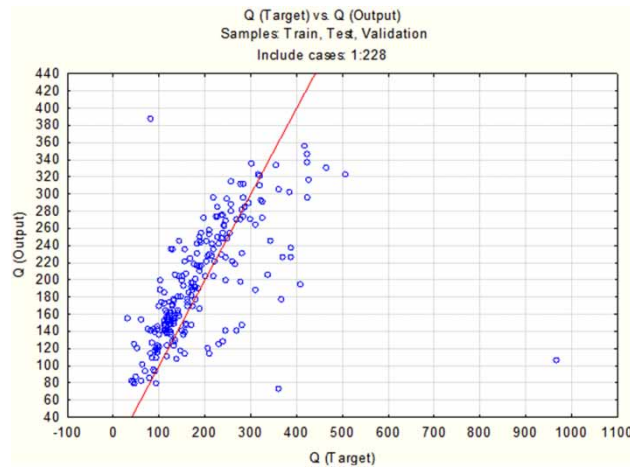


Figure 8 | Comparison between the target and the output streamflow for the ANN model (MLP 1-3-1).

from the selected ANN model (y-axis). It is evident from [Figures 7 and 8](#) that the predictions are not strongly correlated to the original (recorded) data, as prescribed in [Table 1](#). The ANN time series model gave $RMSE = 84.63$ and $R^2 = 0.365$, indicating that it is less efficient than the Box-Jenkins time series model predicted above (which gave $RMSE = 42.049$ and $R^2 = 0.844$). [Figure 9](#) depicts the forecasted monthly streamflow for the 12 months during 2019 (by the ANN time series model), together with the recorded values. The calculated ($RMSE = 93.4$) and the calculated ($R^2 = 0.269$). From this figure, it is evident that the ANN model does not simulate the seasonality of the recorded data. [Figures 6 and 9](#) give an indication that Box-Jenkins models are competent in simulating seasonality, which is not the case for ANN models. Comparing the forecast accuracy ($RMSE$ and R^2) for the ANN model during 2019 with that resulted from the Box-Jenkins model, it is evident that the latter is more accurate. This result is in accordance with the results documented by other authors ([Moeeni et al. 2017](#); [Mehdizadeh et al. 2019](#)). [Figure 10](#) illustrates the future forecasts resulting from the Box-Jenkins model mentioned above by Equations (14) and (15) together with the recorded and fit monthly streamflow for the period 2000–2018. The long-term periodicity is clearly observed; this is in accordance with [Stojković et al. \(2020\)](#).

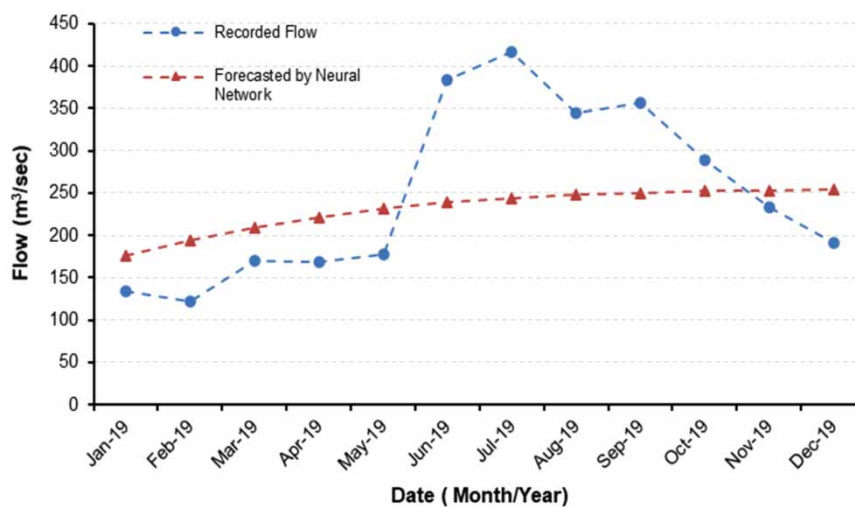


Figure 9 | Recorded vs. Forecasted (by ANN) monthly stream flow during 2019.

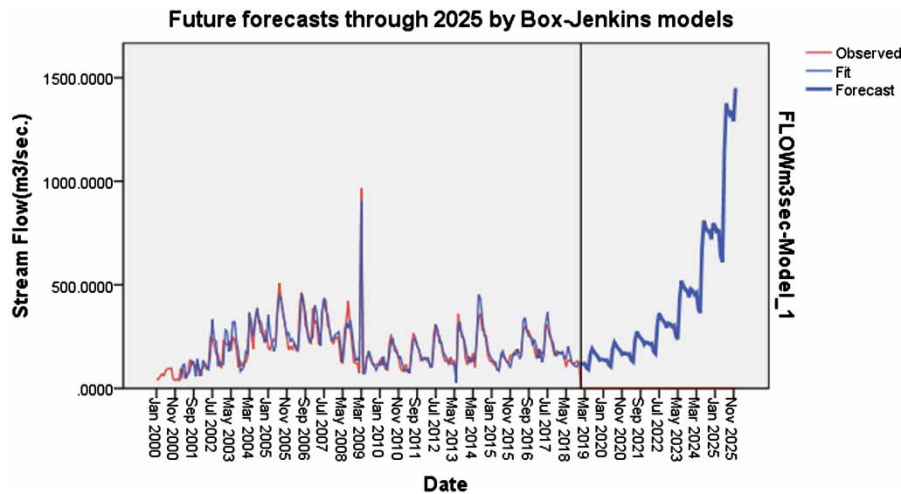


Figure 10 | Future forecasts through 2025 by Box-Jenkins model.

CONCLUSION

From the results of the study, it can be concluded that the Box-Jenkins model was more accurate than the ANN model in forecasting future monthly streamflow downstream of the Euphrates River (Hindiya Barrage)/Iraq for the period 2000–2019, that the ANN model was not able to simulate seasonality, which was not the case for the Box-Jenkins model. Future forecast of monthly streamflow by Box-Jenkins models indicates the existence of some long-period trend in the form of long-term periodicity, which already exists in the recorded data. It is advisable to study the monthly streamflow in terms of the climatic variables through multiple regression and apply the same modeling procedure; that is, the Box-Jenkins (transfer function models) and the ANN (regression models), also the Support Vector Regression and the Random Forest analysis may be adopted in the future studies.

ACKNOWLEDGEMENTS

The authors would like to express their appreciation and gratitude to the Ministry of Higher Education and Scientific Research, Al-Furat Al-Awsat Technical University, and the Ministry of Water Resources/Al-Mussaib Water Resources Directorate/Iraq for the facilities provided to complete this research. The authors are also grateful to the colleagues and the technician team who provided insight and expertise that greatly assisted the completion of the research.

DATA AVAILABILITY STATEMENT

Data cannot be made publicly available; readers should contact the corresponding author for details.

REFERENCES

- Adnan, R. M., Liang, Z., Parmar, K. S., Soni, K. & Kisi, O. 2020 Modeling monthly streamflow in mountainous basin by MARS, GMDH-NN and DENFIS using hydroclimatic data. *Neural Computing Applications* **32**, 1–19.
- Ang, A. H.-S. & Tang, W. H. 2007 *Probability Concepts in Engineering Planning and Design: Emphasis on Application to Civil and Environmental Engineering*. John Wiley & Sons, Hoboken, NJ.
- Avand, M. & Moradi, H. 2020 Using machine learning models, remote sensing, and GIS to investigate the effects of changing climates and land uses on flood probability. *Journal of Hydrology* **63**, 1–15.
- Becerikli, Y., Konar, A. F. & Samad, T. 2003 *Intelligent optimal control with dynamic neural networks*. *Neural Networks* **16**(2), 251–259.

- Bishop, C. M. 1995 *Neural Networks for Pattern Recognition*. Oxford University Press, Oxford, England.
- Box, G. E., Jenkins, G. M., Reinsel, G. C. & Ljung, G. M. 2015 *Time Series Analysis: Forecasting and Control*. John Wiley & Sons, Hoboken, NJ.
- Brown, L. C. & Mac Berthouex, P. 2002 *Statistics for Environmental Engineers*. CRC Press, Boca Raton, FL.
- Faraway, J. & Chatfield, C. 1998 Time series forecasting with neural networks: a comparative study using the air line data. *Journal of the Royal Statistical Society* **47**(2), 231–250.
- Feng, Z.-k. & Niu, W.-J. 2021 Hybrid artificial neural network and cooperation search algorithm for nonlinear river flow time series forecasting in humid and semi-humid regions. *Knowledge-Based Systems* **211**, 1–13.
- Frausto-Solis, J., Pita, E. & Lagunas, J. 2008 Short-term streamflow forecasting: ARIMA vs neural networks. In: *American Conference on Applied Mathematics*, Massachusetts, USA, pp. 402–407.
- Geurts, M. 1977 Time series analysis: forecasting and control. *Journal of Marketing Research* **14**(2), 1–10.
- Joodavi, A., Izady, A., Maroof, M. T. K., Majidi, M. & Rossetto, R. 2020 Deriving optimal operational policies for off-stream man-made reservoir considering conjunctive use of surface and groundwater at the Bar dam reservoir (Iran). *Journal of Hydrology: Regional Studies* **31**, 1–13.
- Kajitani, Y., Hipel, K. W. & McLeod, A. I. 2005 Forecasting nonlinear time series with feed-forward neural networks: a case study of Canadian lynx data. *Journal of Forecasting* **24**(2), 105–117.
- Kawamura, S. 2000 *Integrated Design and Operation of Water Treatment Facilities*. John Wiley & Sons, Hoboken, NJ.
- Khazaei, M. R., Zahabiyou, B. & Hasirchian, M. 2020 A new method for improving the performance of weather generators in reproducing low-frequency variability and in downscaling. *International Journal of Climatology* **40**(12), 5154–5169.
- KIŞI, Ö. & Sciences, E. 2005 Daily river flow forecasting using artificial neural networks and auto-regressive models. *Turkish Journal of Engineering* **29**(1), 9–20.
- Ljung, G. M. & Box, G. E. 1978 On a measure of lack of fit in time series models. *Biometrika* **65**(2), 297–303.
- Mehdizadeh, S., Fathian, F., Safari, M. J. S. & Adamowski, J. F. 2019 Comparative assessment of time series and artificial intelligence models to estimate monthly streamflow: a local and external data analysis approach. *Journal of Hydrology* **579**, 1–13.
- Metcalf, L., Eddy, H. P. & Tchobanoglous, G. 1979 *Tchobanoglous, Wastewater Engineering: Treatment Disposal Reuse*. Tata McGraw Hill, New York, NY.
- Moeeni, H., Bonakdari, H., Fatemi, S. E. & Zaji, A. H. 2017 Assessment of stochastic models and a hybrid artificial neural network-genetic algorithm method in forecasting monthly reservoir inflow. *INAE Letters* **2**(1), 13–23.
- Mohammadi, B., Ahmadi, F., Mehdizadeh, S., Guan, Y., Pham, Q. B., Linh, N. T. T. & Tri, D. Q. 2020 Developing novel robust models to improve the accuracy of daily streamflow modeling. *Journal of Water Resources Management* **34**(10), 3387–3409.
- Niu, W.-J. & Feng, Z.-K. 2021 Evaluating the performances of several artificial intelligence methods in forecasting daily streamflow time series for sustainable water resources management. *Journal of Sustainable Cities Society* **64**, 1–12.
- Peng, F., Wen, J., Zhang, Y. & Jin, J. 2020 Monthly streamflow prediction based on random forest algorithm and phase space reconstruction theory. *IOP Conference Series: Conference Series* **1637**(1), 1–6.
- Stojković, M., Plavšić, J., Prohaska, S., Pavlović, D. & Despotović, J. 2020 A two-stage time series model for monthly hydrological projections under climate change in the Lim River basin (southeast Europe). *Hydrological Sciences Journal* **65**(3), 387–400.
- Tealab, A., Hefny, H. & Badr, A. 2017 Forecasting of nonlinear time series using ANN. *Future Computing and Informatics Journal* **2**(1), 39–47.
- Yaffee, R. A. & McGee, M. 2000 *An Introduction to Time Series Analysis and Forecasting: with Applications of SAS® and SPSS®*. Elsevier, Amsterdam, The Netherlands.
- Zubaidi, S. L., Al-Bugharbee, H., Muhsen, Y. R., Hashim, K., Alkhaddar, R. M. & Hmeesh, W. H. 2019a The prediction of municipal water demand in Iraq: a case study of Baghdad governorate. In: *The 12th International Conference on Developments in ESystems Engineering (DeSE)*, Kazan, Russia, pp. 274–277.
- Zubaidi, S. L., Kot, P., Hashim, K., Alkhaddar, R., Abdellatif, M. & Muhsin, Y. R. 2019b Using LARS-WG model for prediction of temperature in Columbia City, USA. *IOP Conference Series: Materials Science and Engineering* **584**(1), 1–10.
- Zubaidi, S. L., Hashim, K., Ethaib, S., Al-Bdairi, N. S. S., Al-Bugharbee, H. & Gharghan, S. K. 2020a A novel methodology to predict monthly municipal water demand based on weather variables scenario. *Journal of King Saud University-Engineering Sciences* **32**(7), 1–18.
- Zubaidi, S. L., Ortega-Martorell, S., Kot, P., Alkhaddar, R. M., Abdellatif, M., Gharghan, S. K., Ahmed, M. S. & Hashim, K. 2020b A method for predicting long-term municipal water demands under climate change. *Water Resources Management* **34**(3), 1265–1279.
- Zubaidi, S. L., Al-Bugharbee, H., Muhsin, Y. R., Hashim, K. & Alkhaddar, R. 2020c Forecasting of monthly stochastic signal of urban water demand: Baghdad as a case study. *IOP Conference Series: Materials Science and Engineering* **888**(1), 1–7.
- Zubaidi, S. L., Abdulkareem, I. H., Hashim, K. S., Al-Bugharbee, H., Ridha, H. M., Gharghan, S. K., Al-Qaim, F. F., Muradov, M., Kot, P. & Al-Khaddar, R. 2020d Hybridised artificial neural network model with slime mould algorithm: a novel methodology for prediction of urban stochastic water demand. *Water* **12**(10), 1–18.
- Zubaidi, S. L., Ortega-Martorell, S., Al-Bugharbee, H., Olier, I., Hashim, K. S., Gharghan, S. K., Kot, P. & Al-Khaddar, R. 2020e Urban water demand prediction for a city that suffers from climate change and population growth: Gauteng province case study. *Water* **12**(7), 1–18.

First received 29 December 2020; accepted in revised form 2 February 2021. Available online 15 February 2021